



Short Report

Broadening the phenotypic spectrum of POP1-skeletal dysplasias: identification of POP1 mutations in a mild and severe skeletal dysplasia


Barraza-García J., Rivera-Pedroza C.I., Hisado-Oliva A., Belinchón-Martínez A., Sentchordi-Montané L., Duncan E.L., Clark G.R., del Pozo A., Ibáñez-Garikano K., Offiah A., Prieto-Matos P., Cormier-Daire V., Heath K.E. Broadening the phenotypic spectrum of POP1-skeletal dysplasias: identification of POP1 mutations in a mild and severe skeletal dysplasia.

Clin Genet 2017. © John Wiley & Sons A/S. Published by John Wiley & Sons Ltd, 2017

Processing of Precursor 1 (POP1) is a large protein common to the ribonuclease-mitochondrial RNA processing (RNase-MRP) and RNase-P (RMRP) endoribonucleoprotein complexes. Although its precise function is unknown, it appears to participate in the assembly or stability of both complexes. Numerous *RMRP* mutations have been reported in individuals with cartilage-hair hypoplasia (CHH) but, to date, only three *POP1* mutations have been described in two families with features similar to anauxetic dysplasia (AD). We present two further individuals, one with severe short stature and a relatively mild skeletal dysplasia and another in whom AD was suspected. Biallelic *POP1* mutations were identified in both. A missense mutation and a novel single base deletion were detected in proband 1, p.[Pro582Ser]:[Glu870fs*5]. Markedly reduced abundance of RMRP and elevated levels of pre5.8s rRNA was observed. In proband 2, a homozygous novel *POP1* mutation was identified, p.[(Asp511Tyr)];[(Asp511Tyr)]. These two individuals show the phenotypic extremes in the clinical presentation of POP1-dysplasias. Although CHH and other skeletal dysplasias caused by mutations in *RMRP* or *POP1* are commonly cited as ribosomal biogenesis disorders, recent studies question this assumption. We discuss the past and present knowledge about the function of the RMRP complex in skeletal development.

Conflict of interest

The authors have nothing to disclose.

**J. Barraza-García^{a,b,c},
C.I. Rivera-Pedroza^{a,c},
A. Hisado-Oliva^{a,b,c},
A. Belinchón-Martínez^{a,b,c},
L. Sentchordi-Montané^{a,c,d},
E.L. Duncan^e, G.R. Clark^f,
A. del Pozo^{a,b},
K. Ibáñez-Garikano^a, A. Offiah^g,
P. Prieto-Matos^h,
V. Cormier-Daireⁱ
and K.E. Heath^{a,b,c}** 

^aInstitute of Medical & Molecular Genetics (INGEMM), Hospital Universitario La Paz, Universidad Autónoma de Madrid, IdiPAZ, Madrid, Spain, ^bCentro de Investigación Biomédica en Red de Enfermedades Raras (CIBERER), Instituto Carlos III, Madrid, Spain,

^cMultidisciplinary Skeletal dysplasia Unit (UMDE), Hospital Universitario La Paz, Madrid, Spain, ^dDepartment of Pediatric Endocrinology, Hospital Universitario Infanta Leonor, Madrid, Spain,

^eDepartment of Endocrinology, Royal Brisbane and Women's Hospital, Herston, Australia, ^fHuman Genetics Group, University of Queensland Diamantina Institute, Translational Research Institute, Princess Alexandra Hospital, Brisbane, Australia, ^gRadiology Department, Sheffield Children's Hospital NHS Foundation Trust and Academic Unit of Child Health, University of Sheffield, Sheffield, UK, ^hPediatric Endocrinology Unit, Hospital Universitario de Salamanca, Instituto de Investigación Biomédica de Salamanca, Salamanca, Spain, and

ⁱDepartment of Medical Genetics, Reference Center for Skeletal Dysplasia, INSERM UMR 1163, Laboratory of Molecular and Physiopathological Bases of Osteochondrodysplasia, Paris Descartes-Sorbonne Paris Cité University, AP-HP, Institut Imagine and Hôpital

Universitaire Necker-Enfants Malades,
Paris, France

Key words: anauxetic dysplasia – bone
– POP1 – RMRP – skeletal dysplasia

Corresponding author: Karen Heath,
Institute of Medical & Molecular
Genetics, Hospital Universitario La Paz,
Paseo de la Castellana 261, 28046
Madrid, Spain.

Tel.: +34 91 207 1010x269;

fax: +34 91 207 1040;

e-mail: karen.heath@salud.madrid.org

Received 3 October 2016, revised and
accepted for publication 4 January
2017

In the 2015 nosology of skeletal dysplasias (SD), 436 different dysplasias were classified into 42 groups, associated with alterations in >364 genes (1). Discovery of new genes has considerably increased with the implementation of whole-exome/-genome sequencing and at the same time, next-generation sequencing (NGS)-based diagnostics has become a central tool in improving mutation detection and expanding the phenotypic spectrum of known disorders.

The ribonuclease (RNase) for mitochondrial RNA processing (RMRP) endoribonuclease complex, composed of a RNA subunit and 10 different proteins, has been identified in virtually all eukaryotes (2–6). It is essential for cell viability and appears to have evolved from the RNase-P complex to perform specialized functions (5, 7–12). One of the proteins shared by both complexes is the Processing of Precursor 1 (POP1) homolog RNase P/MRP subunit, a large protein that seems to stabilize RNase-P and RMRP complexes (13). Care must be taken in order to avoid confusion with the PYRIN Domain-only Protein, also called POP1.

The RMRP gene (*RMRP*, MIM 157660), encoding the untranslated RNA subunit was the first non-coding nuclear RNA associated with human disease (14). Currently, we know that alterations in *RMRP* are related to several autosomal recessive SDs with varying severity: mild metaphyseal dysplasia without hypotrichosis (MIM 250460); moderate cartilage-hair hypoplasia (CHH, MIM 250250); and severe anauxetic dysplasia (AD, MIM 607095) (15–18).

CHH is a metaphyseal dysplasia in which the limbs and ribs are mostly affected. There is thickening and shortening of the long bones, with wide, irregular, and partially sclerotic metaphyseal borders of the growth plates. Skeletal alterations are present at birth and are distinguished from other metaphyseal dysplasias by more severe affection of the knee compared to the proximal femur. The spine and skull are generally conserved (17, 19, 20). AD is a severe spondyloepimetaphyseal dysplasia with severe short stature of prenatal onset, very short adult height (less than 1 m), hypodontia, midface hypoplasia and mild intellectual disability. Vertebrae are ovoid with concave dorsal surfaces in the lumbar region

and show delayed bone maturation. Femoral heads and necks are hypoplastic, as well as the iliac bodies. Long bones have irregular mineralization of the metaphyses. The first and fifth metacarpals are short and wide with small, late-ossifying epiphyses and bullet-shaped middle phalanges. A large reduction in the number of chondrocytes in the resting and proliferating zones, with diminished columnization of the hypertrophic zone has also been observed (18, 21, 22).

In 2011, two sisters with a SD similar to AD were described (23). Exome analysis revealed two compound heterozygous *POP1* mutations, a gene previously not associated with any disease. More recently, a homozygous *POP1* mutation was identified in another similarly affected individual and the authors suggested that they should be classified as *POP1*-associated skeletal phenotype AD type 2 (24).

We present two index cases, one with an unknown SD and another in whom AD was suspected, in whom biallelic *POP1* mutations were identified. These two probands show the extremes in clinical presentation of *POP1* mutations, and we then compare them to those reported previously. We also review the available literature about the role of POP1 and its relationship with disease.

Clinical cases

Proband 1

Female of Moroccan origin, born to healthy, non-consanguineous parents. Father's height was 180 cm (0.4 Standard deviations (SDS)) and mother's 164 cm (0.1 SDS). Pregnancy was without complications and the child was delivered at 37.5 weeks by cesarean section, weight 2535 g (–2.3 SDS), body length (BL) 45 cm (–3.1 SDS) and head circumference (HC) 34 cm (–1.4 SDS). Short limbs were noted at birth. Karyotype, biochemical and hormonal studies were normal.

At 4.6 years of age, she weighed 11.8 kg (–2.47 SDS), height 84.4 cm (–5.57 SDS) and HC 51.8 cm (1.7 SDS) (Fig. 2). On physical examination, she had relative macrocephaly, short neck, broad chest, hyperlordosis,

brachydactyly, cubitus valgus with difficulties at extension, and prominent heels (Fig. 2). Psychomotor development was normal.

Radiographic analysis showed mild irregularity of the vertebral end plates with posterior scalloping of the lower lumbar vertebral bodies, delayed ossification, hypoplastic femoral necks and in valgus position, slightly widened iliac angle, irregular metaphyses of distal femur and proximal and distal tibiae, irregular metaphyses and cone-shaped epiphyses of all proximal and middle phalanges, and bullet-shaped middle phalanges (Fig. 1a–j). Clinical and radiological data are summarized in Table S1, Supporting information.

Proband 2

Male of Senegalese origin born to healthy parents. Although consanguinity was denied, both parents were from the same village. Father's height 178 cm (0.09 SDS) and mother's 165 cm (0.15 SDS). Intrauterine growth retardation was noted on ultrasound performed at 24-gestational weeks. He was born at 38 weeks, weight 2210 g (−2.32 SDS), BL 38 cm (−6.83 SDS) and HC 31 cm (−1.9 SDS).

He was first seen at 2 years old; height 59.5 cm (−10.18 SDS), weight 6200 g (−4.73 SDS) and HC 46 cm (−2.73 SDS). He was able to walk with help. Clinical exam revealed major deformities of upper and lower limbs. Radiological analysis (Fig. 1k–q) showed severely delayed bone age. He had tall vertebral bodies with posterior scalloping of the lower lumbar vertebral bodies. The pelvis showed narrow iliac wings with mild flaring of the acetabula. He had short, broad humeri with irregular proximal metaphyses, bowing of the ulna, short femoral necks, coxa vara with vertical orientation of the proximal femoral physes and irregularity and sclerosis of the femoral and tibial metaphyses. Middle phalanges were bullet-shaped. A new radiological analysis at age 7 (Fig. 1o–q), revealed thoracolumbar scoliosis, flared metaphyses with irregular margins in the long bones, cupped distal tibial metaphyses, and chevron deformity of distal femoral epiphyses with premature fusion of the growth plate.

At 6 years, his height was 62.5 cm (−10.99 SDS), weight 7200 g (−4 SDS) and HC 47.5 cm (−3.51 SDS) (Fig. 2). Physical examination revealed sparse and apparently hypopigmented hair, hypodontia, cubitus valgus with flexion contractures of the elbows. His hands were smaller when compared to the limbs, with pointed fingers and small, dysplastic nails. He had hip flexion deformity, kyphosis and prominent heels (Figs. 2 and S1). He has cognitive developmental delay. Brain magnetic resonance imaging (MRI) showed hyperintensity of the subcortical and periventricular white matter associated with non-specific subcortical bitemporal edema (Fig. S2). There were no lactate peaks at spectroscopy. Deficiency of complex I of the mitochondrial respiratory chain was also found in fibroblasts, without an assembly abnormality on the Blue Native Polyacrylamide gel electrophoresis (BN-PAGE). But, no features of mitochondrial disease were found including normal hearing

and eye survey and metabolic screening. A clinical diagnosis of CHH/AD was suspected, based on his extreme short stature, lumbar hyperlordosis and kyphoscoliosis, severe long-bone shortening with irregular metaphyses and deformed epiphyses, and brachydactyly with delayed carpal ossification. The absence of *RMRP* mutations, led to *POP1*-direct sequencing.

Materials and methods

All participants provided informed consent and ethical approval was obtained from the respective institutions. DNA was extracted from all participants and RNA was extracted from proband 1 and parents.

Proband 1, with an unknown SD, was analyzed with a custom-designed targeted NGS panel (SkeletalSeq.V3, 315 SD genes) using SeqCap EZ technology (Roche Nimblegen, Madison, WI, USA) and sequenced on a MiSeq (Illumina, San Diego, CA, USA). In house bioinformatic analysis was performed using: Bowtie2 v2.0; Picard-tools 1.27; Samtools v0.1.19-44428 cd; Bedtools v2.16.1; Isis 2.4.60.8, BWA 0.6.1-r104-tpx, Genome Analysis TK v2.6-5, SnpE 3.5e, dbNSFP v2.7, dbSNP v137, ClinVar and human genomic reference sequence hg19. *POP1*-direct sequencing was undertaken for proband 2 and his parents.

Variants were evaluated with the help of Alamut V2.8 and CADD V1.3 (<http://cadd.gs.washington.edu/>), conservation using GerpN and population databases were consulted for frequency data: Exome Aggregation Consortium (ExAC, <http://exac.broadinstitute.org>), NHLBI-GO Exome Sequencing Project (ESP; <https://esp.gs.washington.edu/drupal/>) and Kaviar (<http://db.systemsbio.net/kaviar>).

To determine the functional impact of the mutated alleles, we measured relative abundance of *RMRP* and unprocessed pre-5.8S rRNA compared to endogenous Glyceraldehyde 3-phosphate dehydrogenase (*GADPH*) in proband 1, her unaffected parents, and age- and sex-matched controls, as previously described (23). All reactions were undertaken in triplicate and three biological replicas were performed.

Results

Compound heterozygous and homozygous *POP1* mutations were identified in probands 1 and 2, respectively (Table S2). In proband 1, a missense mutation in exon 13 and a one base deletion in exon 16 were detected, c.[1744C>T];[2607delC]; p.[Pro582Ser];[Glu870fs*5] (Fig. 3). Both variants are absent from population databases. The missense variant has been recently reported in homozygosity in an individual from Morocco (24). It affects a highly conserved amino acid and *in silico* pathogenicity predictions classify the variant as highly deleterious. This mutation was inherited from the mother. The paternally inherited single base deletion in exon 16 is predicted to result in a premature stop codon.

Gene expression assays showed that patient 1 had a markedly reduced abundance of *RMRP* and elevated levels of pre5.8S rRNA when compared to his

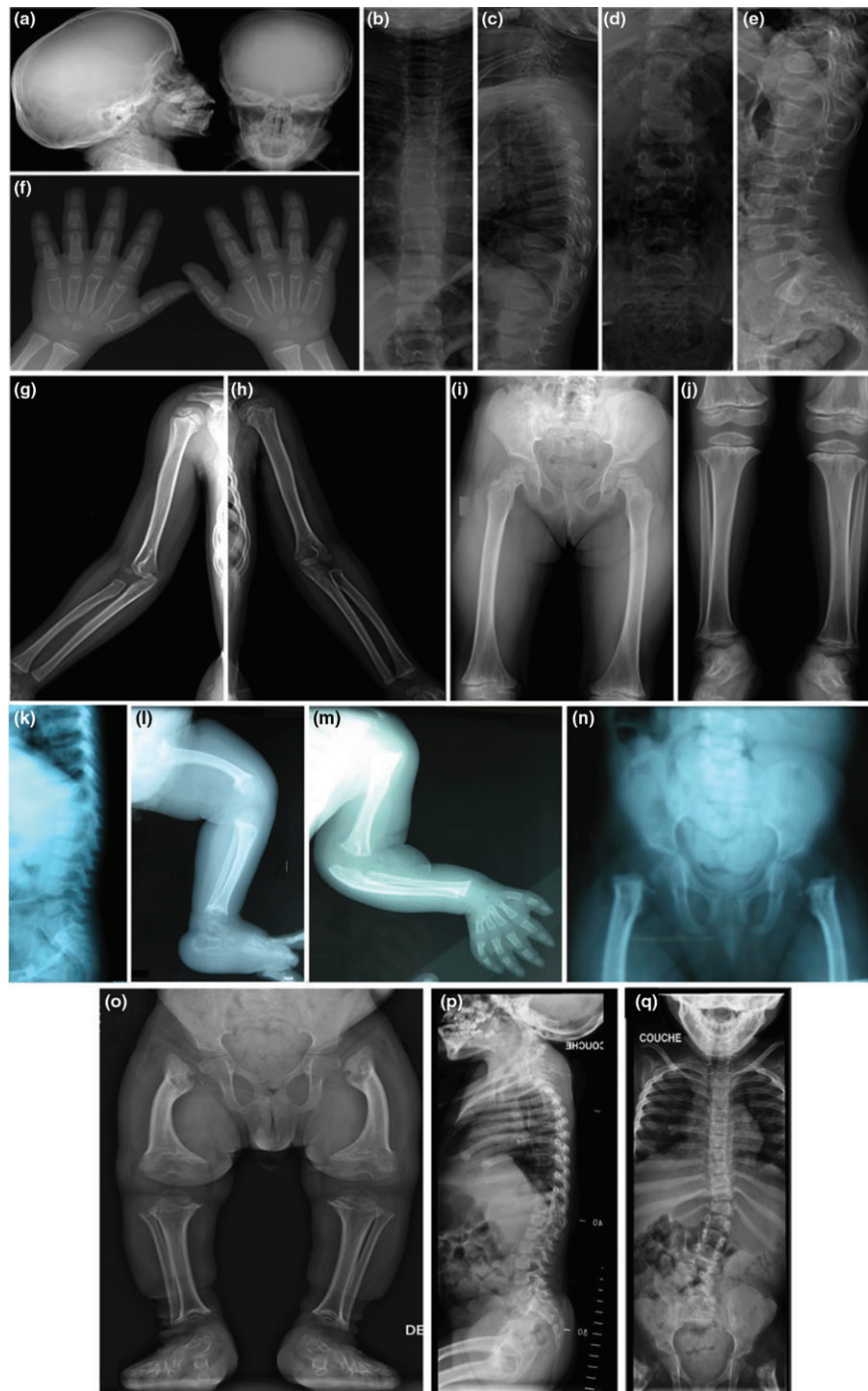


Fig. 1. Radiological analysis of probands 1 and 2. Radiographs of proband 1 at 4.6 years (a)–(j) and proband 2 at age 2 (k)–(n) and 7 years (o)–(q). (a) Macrocephaly, (b) Narrow pedicles, (c) Mild irregularity of vertebral end plates, (d) Narrow pedicles lower thoracic and upper lumbar spine, (e) Posterior scalloping lower lumbar vertebral bodies, (f) Significantly delayed bone age (chronological age = 4.6 years, female SD = 8 m, bone age = 2 years). Cupped, sclerotic, irregular metaphyses of second to fourth metacarpals and all proximal and middle phalanges, cone-shaped epiphyses of proximal and middle phalanges, similar to that in cartilage-hair hypoplasia (CHH), bullet-shaped middle phalanges, ivory epiphysis proximal phalanges fifth fingers and mild proximal pointing of base of second to fifth metacarpals, (g), (h) Patchy linear sclerosis of the proximal humeral metaphyses, (i) Coxa valga. Irregularity and sclerosis of distal femoral metaphyses, (j) irregularity and sclerosis of distal femoral, proximal tibial and distal tibial metaphyses, (k) tall vertebral bodies and posterior scalloping of lower lumbar vertebral bodies, (l) bowed femur. Irregularity and sclerosis of metaphyses of femur and tibia, (m) Short, broad humerus with irregular proximal metaphysis. Bowing of the ulna. Bullet-shaped middle phalanges. Severely delayed bone age with no ossified epiphyses of the hand and wrist (chronological age = 2 years, male SD = 4 m, bone age = birth), (n) Narrow iliac wings with mild flaring of the acetabula. Short femoral necks, coxa vara with vertical orientation of femoral physes and medial fragmentation of the proximal femoral metaphyses, (o) Bilateral coxa vara deformity. Short, broad and bowed femora. Flared metaphyses with irregular margins. Cupped distal tibial metaphyses. Chevron deformity of distal femoral epiphyses with premature fusion of the growth plates, (p), (q). Normal segmentation. Tall vertebral bodies with posterior scalloping of lower thoracic and lumbar vertebral bodies. Thoracolumbar scoliosis centered at T12. Relatively broad ribs.

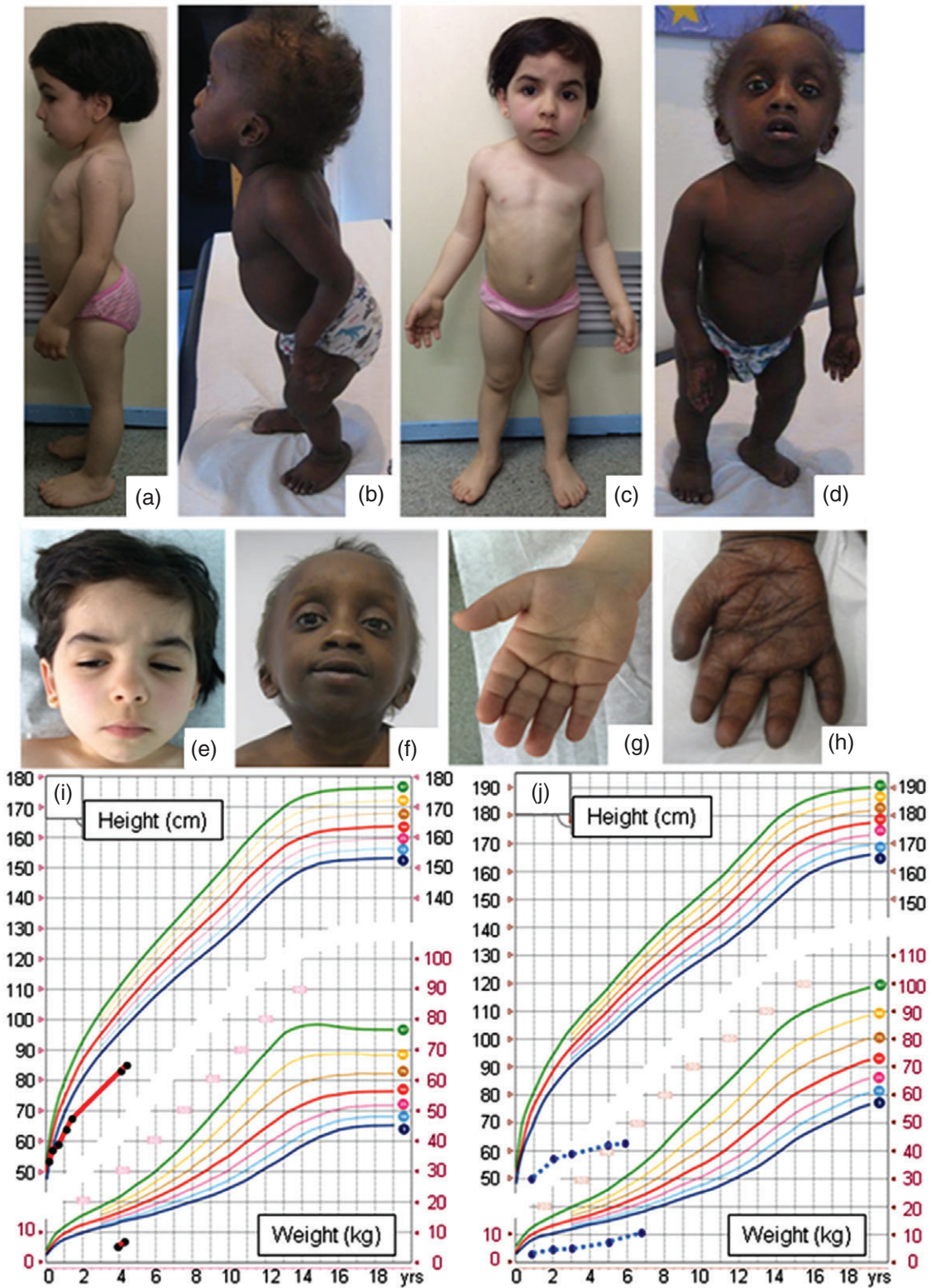


Fig. 2. Clinical photographs and growth curve of the probands. Proband 1 at 4.6 years of age (a, c, e and g): Female individual with relative macrocephaly, short neck, broad chest, hyperlordosis, brachydactyly with stubby fingers, cubitus valgus with difficulties at extension, and prominent heels. Proband 2 at age 5 (b, d) and 7 years of age (f, h): he has sparse and apparently hypopigmented hair. His hands were smaller when compared to his limbs and he had deep palmar creases. He had pointed fingers and his thumbs seemed abnormally located. He also had prominent thorax, hip flexion deformity, kyphosis and prominent heels. The growth curves of proband 1 (i) and proband 2 (j) showing marked growth delay, more severely in proband 2 compared to proband 1.

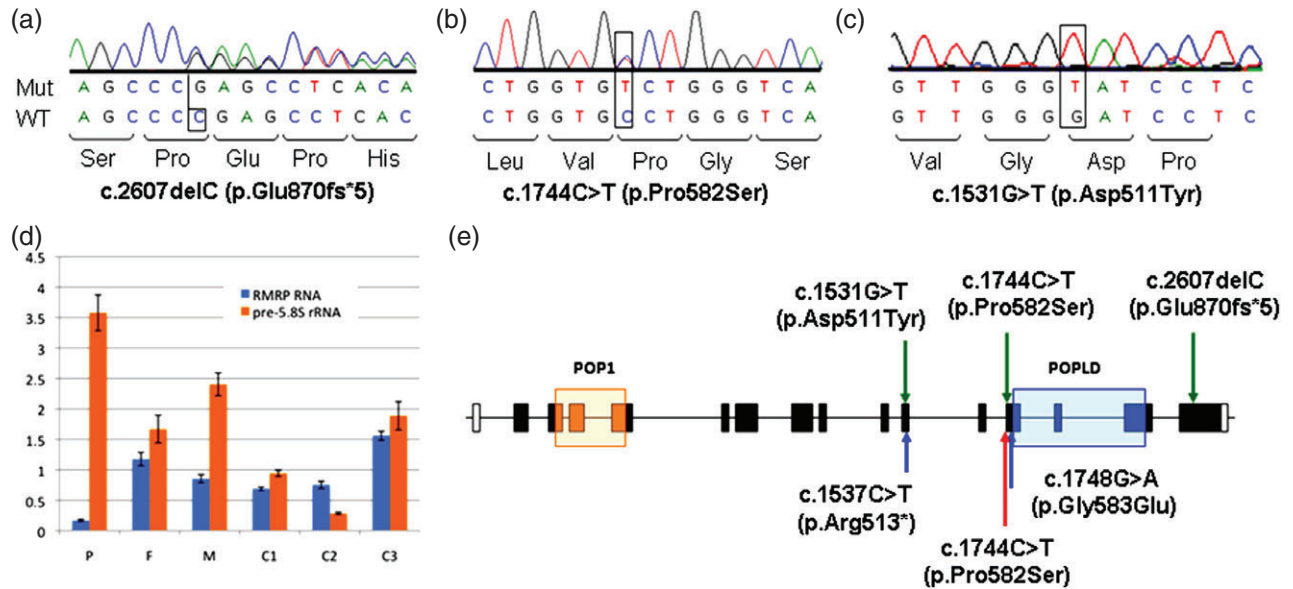


Fig. 3. Genetic characterization of the Processing of Precursor 1 (*POPI*) mutations detected in probands 1 and 2. (a)–(c) Chromatograms of the *POPI* mutations detected in probands 1 (a), (b) and 2 (c). Proband 1 was a compound heterozygote for two *POPI* mutations: c.1744C>T, inherited from the mother, and a single base deletion from his father, c.2607delC. Proband 2 was homozygous for the c.1531G>T mutation. (d) Expression levels of ribonuclease (RNase) for mitochondrial RNA processing (*RMRP*) and pre-5.8S rRNA in proband 1 (P), his mother (M) and father (F) and three unrelated age- and sex-matched controls (C1, C2, and C3). (e): Schematic diagram of *POPI* protein structure showing the localization of the mutations identified in probands 1 and 2 (green arrows) and those previously described mutations, blue arrows [p.(Arg513*);(Gly583Glu), Ref. (23)], red arrows [p.(Pro582Ser);(Pro582Ser), Ref. (24)]. Orange box: *POP1* domain; blue box: *POPLD* domain. Data have been deposited in PhenomeCentral.

unaffected parents and age- and sex-matched controls (Fig. 3).

A homozygous mutation was found in exon 11 of *POPI* in patient 2: c.[1531G>T];[1531G>T]; p.[(Asp511Tyr)];[(Asp511Tyr)] and in heterozygosity in the unaffected parents (Fig. 3). This missense mutation affects a highly conserved amino acid, absent from the population databases and is classified as pathogenic by all *in silico* predictors.

Discussion

In this work, biallelic *POPI* mutations have been identified in two children with a SD with different degrees of severity. Proband 1 is a compound heterozygote for a missense and a frameshift mutation. Interestingly, the p.Pro582Ser mutation has been recently reported in homozygosity in a Moroccan individual with AD-like features (24). As proband 1 is also of Moroccan origin, the two individuals probably share a common ancestor. However, the clinical and radiological data for proband 1 were less severe thus, we did not suspect AD. However, retrospectively, her skeletal findings are very similar, although milder, to the three previously described cases (23, 24).

In contrast, AD was directly suspected in proband 2 but, when no pathogenic mutations were found in *RMRP* and given the previous report of *POPI* mutations in AD type 2, *POPI* was considered as a good candidate gene. Indeed, direct sequencing identified a homozygous *POPI* mutation. This patient has clinical features common to CHH such as hypodontia, sparse and

hypopigmented hair, but also additional features, such as cognitive delay, forearm and hand abnormalities, and brain abnormalities, observed by MRI.

Thus, to date, five different *POPI* mutations have been reported in five individuals from four families (this study, 24, 25) (Fig. 3). Two mutations, a missense and a nonsense, are located in exon 11, codons 511 and 513, in a highly conserved region between the *POP1* and *POPLD* domains. The nonsense mutation is predicted to result in a mutant protein lacking the *POPLD* domain. Another two missense mutations are located in exon 13, encoding Pro582 and Gly583 in the *POPLD* domain. Interestingly, the proximal Ser584 is one of four amino acids shown to be phosphorylated (25). The most C-terminal mutation is located in the last exon, exon 16, and results in the premature truncation of the protein which is unlikely to be exposed to nonsense mediated decay. Although this mutant protein contains both *POP1* domains, its loss of function may be due to a conformational defect. It is noteworthy that, although proband 2 has a missense mutation located very close to the previously reported nonsense variant (23), his phenotype appears to be much more severe.

We compared available clinical and radiological data of the three previous individuals with the two cases described in this study (Table S1). Intrauterine growth restriction was noted in three of five cases, all going on to have shortened BL. Severe postnatal growth retardation was identified in all cases. Involvement of the epiphysis and metaphysis of the long bones and various vertebral bodies abnormalities were described in all individuals (Table S1), bullet-shaped phalanges were identified in

four individuals, involvement of the pelvic bones was noted in three cases, and two had coxa vara. Finally, in all patients except patient 1, the initial suspected diagnosis was AD. Joint laxity, described in some patients with AD, was only observed in one patient while, probands 1 and 2 had limited extension of the elbows.

Attempts to characterize the function of yeast Pop1 *in vitro* have not been successful, mainly due to its insolubility (26). Mutagenizing four evolutionarily conserved Pop1 regions and examining the effects of these mutations on the function and biogenesis of RNase-P and MRP *in vivo* showed that many affect processing of one or more of the precursors of tRNA and the 5.8S rRNA in yeast, suggesting that the mutated positions have similar roles in the functions of the RNase-P/MRP (4, 7, 26–29). *Pop1* mutations have also been shown to be implicated in holoenzyme assembly, leading to destabilization of the RNA component, producing substrate-processing defects in both the RNase-P/MRP (26, 29). These studies explain why CHH and other skeletal dysplasias (SD) caused by mutations in the RNA of RMRP or *POP1* are commonly cited as diseases with alterations in ribosomal biogenesis [reviewed in Ref. (20)]. However, recent studies have laid doubt on these assumptions. When *POP1* was depleted in HeLa cells using interference RNA (RNAi), the levels of pre-rRNA intermediate or in the rate 5.8SS/5.8SL were not significantly altered (30). Furthermore, mature rRNA levels were not significantly affected by the depletion of *POP1*, and, most importantly, there was no change in 5.8S species (30, 31). However, increased levels of 5.8S rRNA precursor have been found in patient 1, the two previously reported siblings with *POP1* mutations (23), and in CHH patients (18). Thus, further studies will be required to clarify the function of *POP1*.

In proband 2, the deficiency of complex I of the respiratory chain was an unexpected finding. The RNase-MRP complex was originally identified in murine cells by its ability to process an RNA transcript complementary to the light strand to generate RNA primers for the heavy-strand DNA replication *in vitro*. Currently, there is discussion about whether RMRP exerts some function in the human mitochondria. It has been shown that mitochondria of a HeLa cell contain 6–15 RMRP RNA molecules and not more than 175 molecules of RNase-P RNA, amounts too low to be functionally relevant (32, 33). This would suggest that RNase-P/MRP complexes reside exclusively in the nuclear compartment, and the mitochondrial activities are associated with other complexes (34, 35).

Mitochondrial disease features, such as complex I deficiency, have not been previously reported in individuals with *POP1* or *RMRP* mutations. This may be a coincidental finding and due to a mutation in another gene. Alternatively, the complex I deficiency could be related to the homozygous *POP1* mutation and be one of the first reports of an association between SD and mitochondrial impairment. However, none of the known functions of *POP1* can explain this observation, thus it will be interesting to investigate if

there is a functional connection. Recently another protein, mitochondria-associated granulocyte-macrophage colony-stimulating factor signalling molecule (MAGMAS), involved in the importing of pre-proteins into the mitochondria and essential for cell growth and development, has been linked with a severe spondylodysplastic dysplasia (36).

Other functions of the RMRP complex may provide an insight into the molecular pathology of *RMRP*- and *POP1*-associated dysplasias. It is known that mRNA levels of cyclin B2 are regulated by RMRP, and that degradation of cyclin B can regulate the cell cycle (37, 38).

RMRP/Telomerase reverse transcriptase (TERT) complexes have also been localized, mainly to the nucleus of cells expressing telomerase (39, 40). RNA RMRP-TERT complexes produce double-stranded RNA that are processed by Dicer to produce siRNAs, which may target genes implicated in skeletal developmental, hair development, and hematopoietic differentiation among others; suggesting that the altered production of siRNA may be the primary pathogenic mechanism in CHH. However, it is the RNA subunit of RNase-MRP that interacts with the complex TERT and not the protein subunits of the complex, so this link may not extend to *POP1* associated dysplasias.

Increased viperin expression has also been observed in patients with CHH and *in vivo* when RMRP and its complex subunits, including *POP1*, are knocked down by RNAi (30, 41). Viperin mRNA is a substrate for cleavage activity of the RNase-MRP complex. Recently, viperin expression has been observed in murine chondrocytes during several developmental stages, and may act as a chondrogenic regulator (41).

In summary, *POP1* mutations have been identified in two individuals with SDs of different severity, expanding the phenotypic spectrum of *POP1*-associated AD type 2. *POP1* mutations should be considered in AD patients without *RMRP* mutations. Our description of a milder phenotype may lead to the identification of additional cases. Finally, further research into the functions of the RMRP complex and *POP1* is needed, to define the molecular mechanism of these SDs.

Supporting Information

Additional supporting information may be found in the online version of this article at the publisher's web-site.

Acknowledgements

This work was supported in part by the following grants: MINECO (SAF2015-66831-R, SAF2012-30871) and the Comunidad de Madrid (ENDOSCREEN: S2010/BMD-2396). J. B.-G. was a recipient of a predoctoral CIBERER fellowship and A. H.-O. was a recipient of a FPI Ph.D. studentship from the Basque Country. We would like to thank the INGEMM NGS and Sequencing Cores for their technical help. We also thank Andreas Zankl and Matthew Brown for their scientific support.

References

- Bonafé L, Cormier-Daire V, Hall C et al. Nosology and classification of genetic skeletal disorders: 2015 revision. *Am J Med Genet A* 2015; 167 (12): 2869–2892.
- Chang DD, Clayton DA. A novel endoribonuclease cleaves at a priming site of mouse mitochondrial DNA replication. *EMBO J* 1987; 6 (2): 409–417.
- Clayton DA. A nuclear function for RNase MRP. *Proc Natl Acad Sci USA* 1994; 91: 4615–4617.
- Lygerou Z, Pluk H, van Venrooij WJ, Séraphin B. hPop1: an autoantigenic protein subunit shared by the human RNase P and RNase MRP ribonucleoproteins. *EMBO J* 1996; 15 (21): 5936–5948.
- Chamberlain JR, Lee Y, Lane WS, Engelke DR. Purification and characterization of the nuclear RNase P holoenzyme complex reveals extensive subunit overlap with RNase MRP. *Genes Dev* 1998; 12 (11): 1678–1690.
- Fagerlund RD, Perederina A, Berezin I, Krasilnikov AS. Footprinting analysis of interactions between the largest eukaryotic RNase P/MRP protein Pop1 and RNase P/MRP RNA components. *RNA* 2015; 21 (9): 1591–1605.
- Lygerou Z, Mitchell P, Petfalski E, Séraphin B, Tollervey D. The POP1 gene encodes a protein component common to the RNase MRP and RNase P ribonucleoproteins. *Genes Dev* 1994; 8 (12): 1423–1433.
- Schmitt ME, Clayton DA. Nuclear RNase MRP is required for correct processing of pre-5.8S rRNA in *Saccharomyces cerevisiae*. *Mol Cell Biol* 1993; 13 (12): 7935–7941.
- Chu S, Zengel JM, Lindahl L. A novel protein shared by RNase MRP and RNase P. *RNA* 1997; 3 (4): 382–391.
- Dichtl B, Tollervey D. Pop3p is essential for the activity of the RNase MRP and RNase P ribonucleoproteins in vivo. *EMBO J* 1997; 16 (2): 417–429.
- Stolc V, Altman S. Rpp1, an essential protein subunit of nuclear RNase P required for processing of precursor tRNA and 35S precursor rRNA in *Saccharomyces cerevisiae*. *Genes Dev* 1997; 11 (21): 2926–2937.
- Salinas K, Wierzbicki S, Zhou L, Schmitt ME. Characterization and purification of *Saccharomyces cerevisiae* RNase MRP reveals a new unique protein component. *J Biol Chem* 2005; 280 (12): 11352–11360.
- Esakova O, Perederina A, Berezin I, Krasilnikov AS. Conserved regions of ribonucleoprotein ribonuclease MRP are involved in interactions with its substrate. *Nucleic Acids Res* 2013; 41 (14): 7084–7091.
- Morrissey JP, Tollervey D. Birth of the snoRNPs: the evolution of RNase MRP and the eukaryotic pre-rRNA-processing system. *Trends Biochem Sci* 1995; 20 (2): 78–82.
- Ridanpää M, van Eenennaam H, Pelin K et al. Mutations in the RNA component of RNase MRP cause a pleiotropic human disease, cartilage-hair hypoplasia. *Cell* 2001; 104 (2): 195–203.
- Kuijpers TW, Ridanpää M, Peters M et al. Short-limbed dwarfism with bowing, combined immune deficiency, and late onset aplastic anaemia caused by novel mutations in the RMPR (sic) gene. *J Med Genet* 2003; 40: 761–766.
- Bonafé L, Dermitzakis ET, Unger S et al. Evolutionary comparison provides evidence for pathogenicity of RMRP mutations. *PLoS Genet* 2005; 1 (4): e47.
- Thiel CT, Horn D, Zabel B et al. Severely incapacitating mutations in patients with extreme short stature identify RNA-processing endoribonuclease RMRP as an essential cell growth regulator. *Am J Hum Genet* 2015; 77 (5): 795–806.
- Mäkitie O, Marttinen E, Kaitila I. Skeletal growth in cartilage-hair hypoplasia. A radiological study of 82 patients. *Pediatr Radiol* 1992; 22 (6): 434–439.
- Trainor PA, Merrill AE. Ribosome biogenesis in skeletal development and the pathogenesis of skeletal disorders. *Biochim Biophys Acta* 2014; 1842 (6): 769–778.
- Menger H, Mundlos S, Becker K, Spranger J, Zabel B. An unknown spondylo-meta-epiphyseal dysplasia in sibs with extreme short stature. *Am J Med Genet* 1996; 63 (1): 80–83.
- Horn D, Rupprecht E, Kunze J, Spranger J. Anauxetic dysplasia, a spondylometaepiphyseal dysplasia with extreme dwarfism. *J Med Genet* 2001; 38: 262–265.
- Glazov EA, Zankl A, Donskoi M et al. Whole-exome re-sequencing in a family quartet identifies POP1 mutations as the cause of a novel skeletal dysplasia. *PLoS Genet* 2011; 7 (3): e1002027.
- Elalaoui SC, Laarabi FZ, Mansouri M, Mrani NA, Nishimura G, Sefiani A. Further evidence of POP1 mutations as the cause of anauxetic dysplasia. *Am J Med Genet* 2016; 170 (9): 2462–2465.
- Matsuoka S, Ballif BA, Smorzorzewska A et al. ATM and ATR substrate analysis reveals extensive protein networks responsive to DNA damage. *Science* 2007; 316 (5828): 1160–1166.
- Xiao S, Hsieh J, Nugent RL, Coughlin DJ, Fierke CA, Engelke DR. Functional characterization of the conserved amino acids in Pop1p, the largest common protein subunit of yeast RNases P and MRP. *RNA* 2006; 12 (6): 1023–1037.
- Pluk H, van Eenennaam H, Rutjes SA, Pruijn GJ, van Venrooij WJ. RNA-protein interactions in the human RNase MRP ribonucleoprotein complex. *RNA* 1999; 5 (4): 512–524.
- Ziehler WA, Morris J, Scott FH, Millikin C, Engelke DR. An essential protein-binding domain of nuclear RNase P RNA. *RNA* 2001; 7 (4): 565–575.
- Welting TJ, van Venrooij WJ, Pruijn GJ. Mutual interactions between subunits of the human RNase MRP ribonucleoprotein complex. *Nucleic Acids Res* 2004; 32 (7): 2138–2146.
- Sloan KE, Mattijssen S, Lebaron S, Tollervey D, Pruijn GJ, Watkins NJ. Both endonucleolytic and exonucleolytic cleavage mediate ITS1 removal during human ribosomal RNA processing. *J Cell Biol* 2013; 200 (5): 577–588.
- Henras AK, Plisson-Chastang C, O'Donohue MF, Chakraborty A, Gleizes PE. An overview of pre-ribosomal RNA processing in eukaryotes. *Wiley Interdiscip Rev RNA* 2015; 6 (2): 225–242.
- Puranam RS, Attardi G. The RNase P associated with HeLa cell mitochondria contains an essential RNA component identical in sequence to that of the nuclear RNase P. *Mol Cell Biol* 2001; 21 (2): 548–561.
- Rossmannith W. Of P and Z: mitochondrial tRNA processing enzymes. *Biochim Biophys Acta* 2012; 1819 (9–10): 1017–1026.
- Mattijssen S, Welting TJ, Pruijn GJ. RNase MRP and disease. *Wiley Interdiscip Rev RNA* 2010; 1 (1): 102–116.
- Powell CA, Nicholls TJ, Minczuk M. Nuclear-encoded factors involved in post-transcriptional processing and modification of mitochondrial tRNAs in human disease. *Front Genet* 2015; 6: 79.
- Mehawej C, Delahodde A, Legeai-Mallet L et al. The impairment of MAGMAS function in human is responsible for a severe skeletal dysplasia. *PLoS Genet* 2014; 10 (5): e1004311.
- Cai T, Reilly TR, Cerio M, Schmitt ME. Mutagenesis of SNM1, which encodes a protein component of the yeast RNase MRP, reveals a role for this ribonucleoprotein endoribonuclease in plasmid segregation. *Mol Cell Biol* 1999; 19 (11): 7857–7869.
- Gill T, Cai T, Aulds J, Wierzbicki S, Schmitt ME. RNase MRP cleaves the CLB2 mRNA to promote cell cycle progression: novel method of mRNA degradation. *Mol Cell Biol* 2004; 24 (3): 945–953.
- Maida Y, Yasukawa M, Furuchi M et al. An RNA-dependent RNA polymerase formed by TERT and the RMRP RNA. *Nature* 2009; 461 (7261): 230–235.
- Jarrous N, Gopalan V. Archaeal/eukaryal RNase P: subunits, functions and RNA diversification. *Nucleic Acids Res* 2010; 38 (22): 7885–7894.
- Steinbusch MM, Caron MM, Eckmann F et al. Viperin: A novel chondrogenic regulator. *Osteoarthritis Cartilage* 2015; 23 (2): A148–A149.